Nonvolatile two-color holographic recording in near-stoichiometric lithium niobate crystals gated by incoherent ultraviolet light

Shaolin Chen (陈绍林)[1], Xiangming Liu (刘祥明)[1,2], Bo Fu (付 博)[3], and Guoquan Zhang (张国权)[1,2*]

[1] *The Key Laboratory of Weak Light Nonlinear Photonics, Ministry of Education of China, Nankai University, Tianjin 300457*

[2] *Photonics Center, College of Physics Science, Nankai University, Tianjin 300071*

[3] *Institute of Fluid Physics, China Academy of Engineering Physics, Mianyang 621900*

[*] *E-mail: zhanggq@nankai.edu.cn*

Received May 30, 2008

Nonvolatile two-color holographic recording gated by incoherent ultraviolet (UV) light centered at 365 nm is investigated in near-stoichiometric lithium niobate crystals. The influence of thermal treatment on the two-color recording is studied. The results show that thermal reduction tends to improve the two-color recording performance, whereas thermal oxidation degrades the two-color recording. With an incoherent 0.2-W/cm^2 UV gating light and a 0.25-W/cm^2 semiconductor recording laser at 780 nm, a two-color recording sensitivity of 4×10^{-3} cm/J and a recording dynamic range characterized by M/# of 0.12 are achieved in a 2.2-mm thermally reduced near-stoichiometric lithium niobate crystal. We attribute the improvement to the prolonged lifetime of small polarons and the increased absorption at the gating wavelength due to thermal reduction.

OCIS codes: 210.2860, 090.2900, 160.2900, 160.5320.

doi: 10.3788/COL20090701.0067.

Nonvolatile two-color holographic recording has been intensively studied in photorefractive materials such as lithium niobate ($LiNbO_3$) and lithium tantalite ($LiTaO_3$) crystals[1]. Early studies on two-color holography employed high-intensity laser pulses as gating and recording lights[2,3]. Nevertheless, from the viewpoint of practical applications, nonvolatile two-color holographic recording with low-intensity lights or even incoherent lights are highly desired. Significant progress has been made and various ways have been proposed to achieve nonvolatile two-color holography at low light intensities recently. Buse *et al.* interpreted the two-color recording process in $LiNbO_3$ as a two-center model[3]. Bai *et al.* demonstrated two-color holography via a long-lived intermediate state in $LiNbO_3$ with relatively low-intensity continuous-wave lasers[4,5]. Soon after, the intermediate state in $LiNbO_3$ was attributed to the small polarons formed at the anti-site defect Nb_{Li}. The small polarons play a key role in the realization of two-color holography[6−9]. In particular, the lifetime of small polarons in $LiNbO_3$ is crucial for the performance of two-color holography as far as the two-color recording sensitivity and the dynamic range are considered. It is found that the lifetime of small polarons in near-stoichiometric $LiNbO_3$ increases owing to the reduced electron-phonon coupling[7,10]. For this reason, the recording sensitivity in near-stoichiometric $LiNbO_3$ can be improved significantly. Nonvolatile two-color holography has also been realized in the intentionally doubly doped $LiNbO_3$ crystals[11−15] such as $LiNbO_3$:Fe,Mn and $LiNbO_3$:Ce,Cu. Here the two external dopants serve as the deep and the shallow centers for the two-color holography.

In this letter, we report the nonvolatile two-color holographic recording performance of the thermally treated near-stoichiometric $LiNbO_3$ crystals by using incoherent ultraviolet (UV) light as gating beam and a 780-nm semiconductor laser as recording beam. The results show that high recording sensitivity and large dynamic range can be achieved by gating the near-stoichiometric $LiNbO_3$ with low-intensity incoherent UV lights.

The near-stoichiometric $LiNbO_3$ crystals were grown by adding 6 wt.-% K_2O into the congruent melt using the Czochralski method[16]. Three y-cut near-stoichiometric $LiNbO_3$ crystal sheets with different thermal treatments were prepared from the same crystal boule: the first was an as-grown one (named as SLN), the second one was oxidized in air for 6 h at 745 °C (named as SLNO), and the third one was reduced in argon atmosphere for 3 h at 745 °C (named as SLNR). All samples were of 2.2-mm thickness. The Li/Nb ratio in the crystal was measured to be 0.985 by using the Raman linewidth of the phonon A_1 mode at 876 cm^{-1} of $LiNbO_3$[16]. Figure 1 shows the absorption spectra of the three samples. It is seen that the absorption in the visible and near-UV spectral regions increases due to the thermal reduction, whereas it decreases after the thermal oxidation.

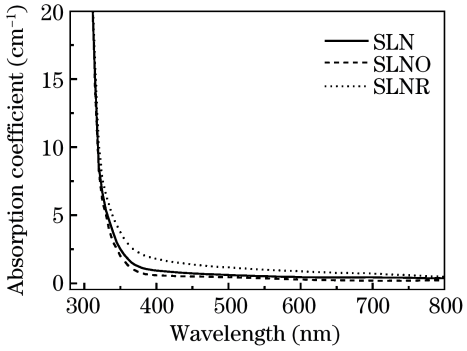

Fig. 1. Linear absorption spectra for SLN, SLNO, and SLNR.

Two-color recording was performed using an incoherent UV light centered at 365 nm as the gating light and a 780-nm semiconductor laser as the recording beam. The recording wavelength was set to be 780 nm because the absorption of the small polarons in $LiNbO_3$ was peaked at ~ 780 nm[17], therefore high recording sensitivity was expected. Two coherent 780-nm recording beams of equal intensity were used to record holographic gratings, the grating vector was along the c-axis of the crystal, and the grating spacing Λ was set to be 1.4 μm. The UV gating beam and the two recording beams were simultaneously on at the beginning of the recording stage. During the recording stage, one of the recording beams was chopped from time to time so that the other recording beam could be used as a readout beam to monitor the grating buildup process. The diffraction efficiency η of the gratings was defined as the intensity ratio of the diffracted beam to the sum of the diffracted and the transmitted beams of the readout beam during the readout interval. During the fixing stage of two-color holographic cycle, the UV gating beam and one of the recording beams were switched off, while the other recording beam served as the fixing beam (as well as the readout beam). The gratings could be finally erased by the UV incoherent light during the erasing stage. Figure 2 shows the typical temporal evolution of the two-color holographic recording cycles including the recording, fixing, and erasing stages for the three samples SLN, SLNO, and SLNR, respectively. The total recording intensity I_r is 0.25 W/cm^2, the grating spacing Λ is 1.4 μm, and the UV gating intensity I_{UV} is 0.16 W/cm^2. It is seen that nonvolatile readout can be achieved in all samples although the diffraction efficiency η decreases slightly during the one-hour continuous readout for SLNR, which is because the thermal reduction induces weak photorefractive sensitivity at 780 nm in SLNR.

Figure 3 shows the dependence of the two-color recording sensitivity on the gating intensity with a total recording intensity $I_r = 0.25$ W/cm^2 and a grating spacing $\Lambda = 1.4$ μm. The two-color recording sensitivity is defined as $S = \left(\partial\sqrt{\eta}/\partial t\right)|_{t=0}/(I_r d)$, where $\partial\sqrt{\eta}/\partial t\big|_{t=0}$ denotes the initial slope of the square root of the diffraction efficiency and d is the thickness of the crystal. As expected, the sensitivity S increases linearly with the increment of the gating intensity I_{UV} in all samples. It is evident from Fig. 3 that S decreases after the thermal oxidation, whereas it increases with the thermal reduction. A recording sensitivity as high as $\sim 4\times10^{-3}$ cm/J was achieved with a gating intensity of 0.2 W/cm^2 for SLNR.

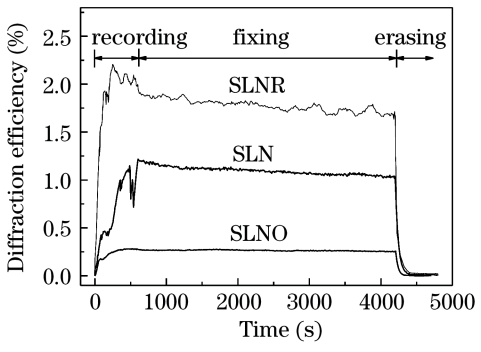

Fig. 2. Typical temporal evolution of two-color recording cycles including the recording, fixing, and erasing stages for SLN, SLNO, and SLNR. The experimental parameters for Λ, I_r, and I_{UV} are 1.4 μm, 0.25 W/cm^2, and 0.16 W/cm^2, respectively.

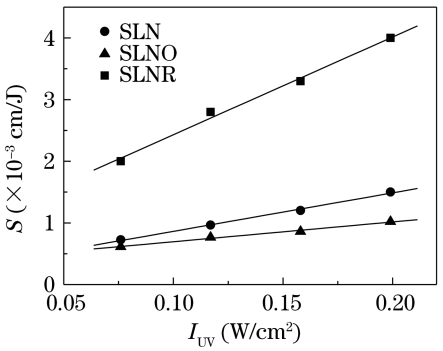

Fig. 3. Dependences of the sensitivity S on the gating intensity I_{UV} for SLN, SLNO, and SLNR. The lines are the least-square linear fit to the measured data. The experimental parameters for Λ and I_r are 1.4 μm and 0.25 W/cm^2, respectively.

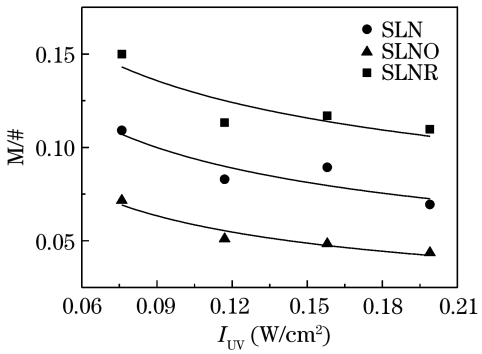

Fig. 4. Dependences of the dynamic range M/# on the UV gating intensity for SLN, SLNO, and SLNR. The curves are guided by the experimental data. The experimental parameters for Λ and I_r are 1.4 μm and 0.25 W/cm^2, respectively.

Figure 4 shows the dynamic range characterized by M/#[18] as a function of the gating intensity with a total recording intensity $I_r = 0.25$ W/cm^2 and a grating spacing $\Lambda = 1.4$ μm. Here M/# is defined as $\tau_e\left(\partial\sqrt{\eta}/\partial t\right)\big|_{t=0}$, where τ_e is the erasing time constant of the gratings during the erasing stage (see Fig. 2). M/# decreases slightly with the increment of the gating intensity because of the erasing effect of the gating beam. Again, the results show that M/# improves after the thermal reduction, whereas it degrades with the thermal oxidation. The M/# value is ~ 0.15 at a gating intensity of 0.075 W/cm^2. An M/# value of ~ 2.7 is expected for SLNR with a recording intensity of 1 W/cm^2 and a crystal thickness of 1 cm since M/# is proportional to the product of the recording intensity and the crystal thickness[6].

It is seen that thermal reduction can effectively improve the two-color recording performance such as the recording sensitivity and the dynamic range. One reason for this improvement is the increased absorption at the gating wavelength after the thermal reduction, as seen from Fig. 1. Therefore, more electrons are photo-excited to the conduction band and then trapped at anti-site

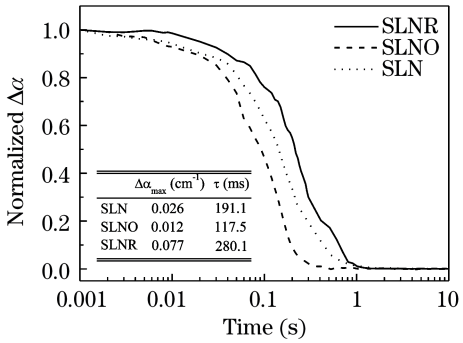

Fig. 5. Dark decay dynamics of the small polarons in SLN, SLNO, and SLNR. The inset table shows the UV-induced absorption coefficient change amplitude $\Delta\alpha_{\max}$ and the dark decay time constant τ for SLN, SLNO, and SLNR, respectively. The probe beam is set at 780 nm of 1 mW/cm^2, and the pump beam is the UV incoherent light of 0.65 W/cm^2.

defects $Nb_{Li}{}^{5+}$, and more small polarons are generated in SLNR. The other reason is the prolonged lifetime of small polarons which also leads to an increase in the UV-induced small polaron concentration in the thermally reduced crystal SLNR. Figure 5 shows the normalized dark decay dynamics of the UV-induced absorption changes at 780 nm. The intensity of the UV pump light is 0.65 W/cm^2, and the probe beam is 1 mW/cm^2 to eliminate the influence on the dark decay dynamics. The inset table shows the UV-induced absorption coefficient change amplitude $\Delta\alpha_{\max}$ and the dark decay time constant τ extracted by using a single exponential decay model of small polarons. $\Delta\alpha_{\max}$ is proportional to the UV-induced small polaron concentration, while τ characterizes the lifetime of small polarons in the near-stoichiometric $LiNbO_3$ crystals. It is seen that the values of $\Delta\alpha_{\max}$ and τ are the largest in SLNR, while they are the smallest in SLNO. This is in accordance with the experimental results on S and M/#.

In summary, we have demonstrated that thermal reduction improves the nonvolatile two-color holographic recording performance of near-stoichiometric $LiNbO_3$ crystals. High recording sensitivity and large dynamic range are achieved in nonvolatile two-color holographic recording in near-stoichiometric $LiNbO_3$ crystals with a low-intensity incoherent UV gating beam. The results may be useful to simplify the nonvolatile two-color storage system.

This work was supported by the National Natural Science Foundation of China (No. 60678021), the Program for New Century Excellent Talents in University (NCET-04-0234), the Program for Changjiang Scholars and Innovative Research Team in University (IRT0149), the Municipal International Cooperation Program of Tianjin (No. 06YFGHHZ00500), the National "973" Program of China (No. 2007CB307002), the Chinese National Key Basic Research Special Fund (No. 2006CB921703), the 111 Project, and the Cultivation Fund of the Key Scientific and Technical Innovation Project, Ministry of Education of China (No. 708022).

References

1. J. Ashley, M.-P. Bernal, G. W. Burr, H. Coufal, H. Guenther, J. A. Hoffnagle, C. M. Jefferson, B. Marcus, R. M. Macfarlane, R. M. Shelby, and G. T. Sincerbox, IBM J. Res. Develop. **44,** 341 (2000).
2. D. von der Linde, A. M. Glass, and K. F. Rodgers, Appl. Phys. Lett. **25,** 155 (1974).
3. K. Buse, F. Jermann, and E. Krätzig, Appl. Phys. A **58,** 191 (1994).
4. Y. S. Bai, R. R. Neurgaonkar, and R. Kachru, Opt. Lett. **22,** 334 (1997).
5. Y. S. Bai and R. Kachru, Phys. Rev. Lett. **78,** 2944 (1997).
6. H. Guenther, R. Macfarlane, Y. Furukawa, K. Kitamura, and R. Neurgaonkar, Appl. Opt. **37,** 7611 (1998).
7. L. Hesselink, S. S. Orlov, A. Liu, A. Akella, D. Lande, and R. R. Neurgaonkar, Science **282,** 1089 (1998).
8. G. Zhang, Y. Tomita, W. Xu, and C. Yang, Appl. Phys. Lett. **77,** 3508 (2000).
9. G. Zhang, S. Sunarno, M. Hoshi, Y. Tomita, C. Yang, and W. Xu, Appl. Opt. **40,** 5248 (2001).
10. O. F. Schirmer, O. Thiemann, and M. Wöhlecke, J. Phys. Chem. Solids **52,** 185 (1991).
11. K. Buse, A. Adibi, and D. Psaltis, Nature **393,** 665 (1998).
12. L. Ren, L. Liu, D. Liu, J. Zu, and Z. Luan, Opt. Lett. **29,** 186 (2004).
13. D. Liu, L. Liu, L. Ren, Z. Luan, and Y. Zhou, Chin. Opt. Lett. **2,** 630 (2004).
14. C. Dai, L. Liu, D. Liu, and Y. Zhou, Chin. Opt. Lett. **3,** 507 (2005).
15. Y. Guo, L. Liu, D. Liu, Z. Chai, and R. Zhu, Acta Opt. Sin. (in Chinese) **26,** 1240 (2006).
16. G. I. Malovichko, V. G. Grachev, E. P. Kokanyan, O. F. Schirmer, K. Betzler, B. Gather, F. Jermann, S. Klauer, U. Schlarb, and M. Wöhlecke, Appl. Phys. A **56,** 103 (1993).
17. L. Arizmendi, J. M. Cabrera, and F. Agulló-López, J. Phys. C **17,** 515 (1984).
18. F. H. Mok, G. W. Burr, and D. Psaltis, Opt. Lett. **21,** 896 (1996).